RSC Advances

PAPER

View Article Online
View Journal | View Issue

Cite this: *RSC Adv.*, 2025, **15**, 11045

Novel heterogeneous Fenton catalysts prepared using electrolytic manganese residue for efficient degradation of acetaminophen†

Hangdao Qin, *[a] Junnan Hao,[a] Yong Wang,[a] Jiming Huang,[a] Jun Chang,[a] Guo Yang,[b] Bo Xing,[b] Sizhan Wu[a] and Jing Chen [a]

Received 4th March 2025
Accepted 26th March 2025

DOI: 10.1039/d5ra01539a

rsc.li/rsc-advances

Electrolytic manganese residue (EMR) was used as a support to prepare novel EMR-supported catalysts for the heterogeneous Fenton degradation of acetaminophen. Among the five supported catalysts, Co/EMR showed the highest catalytic activity. Several important factors influencing the decay of acetaminophen, including Co loading content, catalyst dosage, H_2O_2 concentration and initial solution pH, were investigated. Under optimal experimental conditions, acetaminophen degradation rate and the TOC removal efficiency reached 63.8% and 35.7% within 480 min, respectively. Free radical quenching and EPR analysis showed that the high catalytic degradation rate of acetaminophen could be ascribed to the presence of $^{\bullet}OH$ and $O_2^{\bullet-}$. Based on the XPS analysis, the superior catalytic performance of Co/EMR was attributed to the Fe, Mn and Co active sites and oxygen vacancies (O_v) on the surface. Additionally, the potential for degradation of other pollutants and the applicability in real water matrices as well as the reusability of Co/EMR were investigated. This heterogeneous Fenton system could expand possibilities for high-value utilization of the EMR and showed potential for treating PPCPs in wastewater.

1. Introduction

Acetaminophen, one of the pharmaceutical and personal care products (PPCPs), is a widely used antipyretic and analgesic pharmaceutical, and it can be released into the aquatic environment by human excretion through feces and urine.[1] Water contaminated with acetaminophen has given rise to several health issues in human beings since acetaminophen and its by-products show high toxicity toward kidneys and liver.[2] Hence, it is vitally important to find efficient and practical degradation methods to remove acetaminophen from the aquatic environment.

Fenton system has been proved to effectively eliminate organic pollutants in water due to the catalytic generation of powerful reactive oxygen species (ROS).[3,4] Previous studies have proved that Fe-containing and Mn-containing catalysts are active in facilitating the generation of ROS in the oxidation system.[5–7] Besides, in the previous works of the authors, a bimetallic catalyst $MnFe_2O_4$ has proved to be an effective catalyst for the degradation of antibiotics through a heterogeneous Fenton process.[8–11] Fe and Mn synergistically promoted the production of $^{\bullet}OH$ radicals, which were the main ROS for the decay of antibiotics.

Moreover, it is promising and meaningful to use metallurgical slags as AOP catalysts to "treat waste with waste". Abundant active metals can be found in metallurgical slag materials. For instance, the leaching of Mn in electrolytic manganese residue (EMR) reached 868.6 mg L^{-1}, while 958.8 mg per L Zn and 536.2 mg per L Mn were leached from lead-zinc slag.[12] The existence of active metals in metallurgical slags makes them feasible as a precursor for the preparation of catalysts. On the other hand, substantial amounts of metallurgical slags not only occupy land resources, but also result in significant environmental problems because soil, surface water and groundwater are seriously polluted by the leachate of this slag.[13,14] Although methods for safely disposing or utilizing metallurgical slag materials have been extensively studied, employing these slags as AOP catalysts offers their alternative utilization.

Among these metallurgical slags, the electrolytic manganese industry generates EMR as an acidic solid waste, and producing 1 ton Mn requires about 10–12 tons of EMR.[15] Therefore, strategies for safely treating and utilizing EMR have attracted widespread attention.[16] Methods including the deep extraction and recovery of valuable elements from EMR,[17–19] stabilization/solidification and electrokinetic remediation technologies[20–22] and the use of EMR as a raw material for manufacturing building materials[23–25] have been reported in many literatures. Moreover, EMR was also used to synthesize AOP catalysts for the removal of refractory organic pollutants in wastewater.[26] To

[a]School of Material and Chemical Engineering, Tongren University, Tongren 554300, China. E-mail: qinhangdao@126.com

[b]College of Chemical Engineering, Sichuan University of Science and Engineering, Zigong 643000, China

† Electronic supplementary information (ESI) available. See DOI: https://doi.org/10.1039/d5ra01539a

prepare a novel AOP catalyst, Lan *et al.*[27] treated EMR with EDTA-2Na/NaOH, and then the EMR was ultrasonically etched and hydrothermally treated. The obtained catalyst was used in heterogeneous Fenton reaction for treating synthetic textile wastewater. The results demonstrated that 40 mg per L catalyst, 100 mg per L azo dyes, and 0.4 mM H_2O_2 resulted in an approximately 99% dye removal efficiency. Additionally, a novel heterogeneous catalyst (MS-N3H) was obtained by utilizing EMR as the raw material through the modification of Na_2CO_3 and HNO_3.[28] In combination with PMS, MS-N3H was able to effectively remove levofloxacin from water. The abundant Mn and Fe on the MS-N3H surface as well as lattice oxygen played a crucial role in ROS production.

In this study, EMR was used as a support to prepare heterogeneous Fenton catalysts. The effect of active components supported on EMR was firstly evaluated in the heterogeneous Fenton degradation of acetaminophen. The degradation performance with diverse parameters was investigated to determine the effectiveness of the oxidation system. The reaction conditions including initial pH, H_2O_2 dosages and inorganic anions were optimized. Furthermore, the produced ROS were determined and reasonable catalytic mechanisms were proposed. Finally, the reusability and the applicability of Co/EMR in real water matrices were investigated.

2. Experimental

2.1. Catalyst preparation

The details about the chemicals applied in this work are reported in the ESI (Text S1).†

The used EMR in this study, obtained from Guizhou Sanxiang Technology Co., Ltd (Tongren, China), was treated by an incineration process to remove NH_4^+-N and stabilize sulphur. Distilled water was used to wash the EMR, followed by drying for 12 h at 110 °C before use. The supported catalysts were prepared by an incipient wetness impregnation method using EMR as the support. The EMR was impregnated with different aqueous solutions of $Mn(NO_3)_2\cdot 9H_2O$, $Fe(NO_3)_3\cdot 9H_2O$, $Ce(NO_3)_3\cdot 6H_2O$, $Zn(NO_3)_2\cdot 9H_2O$ and $CoCl_2\cdot 6H_2O$. The Mn/Fe/Ce/Zn/Co loading content was 5%. After impregnation, each obtained catalyst underwent drying for 12 h at 110 °C, followed by calcination in a muffle furnace at a certain temperature for 3 h using a ramp rate of 10 °C min^{-1} to obtain Mn/EMR, Fe/EMR, Ce/EMR, Zn/EMR and Co/EMR.

2.2. Catalyst characterization

The detailed information including instruments and methods used in catalyst characterization is reported in the ESI (Text S2).†

2.3. Removal experiments

Acetaminophen adsorption and heterogeneous Fenton degradation were studied under a constant temperature of 25 °C using a 250 mL conical flask as the reaction vessel. A constant temperature air bath shaker (300 rpm) was used to regulate the temperature. The flask was filled with 100 mL of acetaminophen solution (10 mg L^{-1}), followed by the addition of a certain mass of the solid catalyst. Then a desired amount of H_2O_2 was introduced into the system to initiate the heterogeneous Fenton reaction, while pure adsorption experiments were conducted without H_2O_2 addition. To evaluate the reaction progress, samples were extracted at specific time intervals, and a 0.45 μm membrane was used to immediately filter each sample prior to analysis.

2.4. Analytical methods

A high performance liquid chromatograph (HPLC, LC-20AD XR, Shimadzu) with a C18 column (4.6 × 250 mm, 5 μm) and a PDA detector was utilized for quantitative acetaminophen concentration analysis. A 20 μL injection volume, 243 nm detector wavelength, and mixed acetonitrile and deionized water (50 : 50, v/v) mobile phase with a 0.8 mL min^{-1} flow rate were employed. Total organic carbon analysis (Shimadzu, TOC-L CPN) was employed to study pollutant mineralization.

3. Results and discussion

3.1. Characterization

XRD patterns of EMR and EMR-supported catalysts are displayed in Fig. 1. $CaSO_4\cdot 2H_2O$ (JCPDS No. 21-0816) and SiO_2 (JCPDS No. 46-1054) were identified as the main EMR phases. In the curves of EMR-supported catalysts, the characteristic diffraction peaks corresponding to $CaSO_4$ (JCPDS No. 337-0184) at 25.4° apparently appeared, which could be due to the loss of the crystal water in the $CaSO_4\cdot 2H_2O$ molecule during the calcination process. It is worth noting that the characteristic diffraction peaks of all active components could not be found, which suggested that these metal oxide particles were small and well dispersed on the surface of EMR.

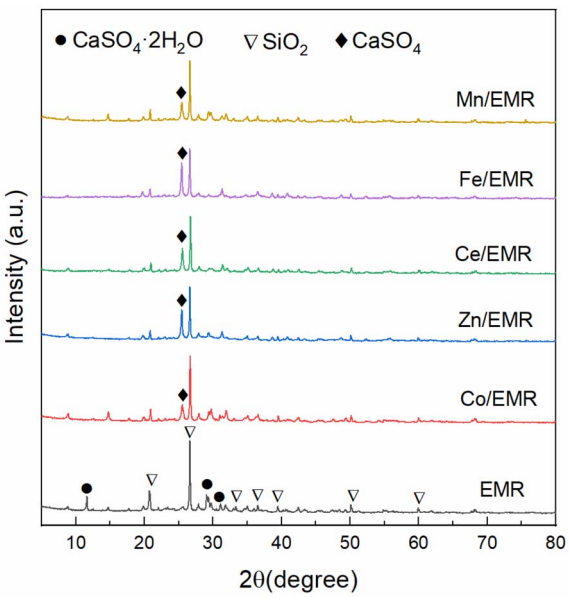

Fig. 1 XRD patterns of EMR and EMR-supported catalysts.

Table 1 Textural characteristics of the catalysts

Sample	BET surface area (m^2 g^{-1})	Pore volume (cm^3 g^{-1})	Average pore size (nm)
EMR	34	0.089	10.6
Mn/EMR	18	0.073	14.1
Fe/EMR	10	0.061	18.8
Ce/EMR	25	0.075	10.2
Zn/EMR	18	0.073	15.7
Co/EMR (5%)	15	0.072	16.4
Co/EMR (9%)	9	0.048	17.5

N_2 adsorption–desorption isotherms were used to determine the BET surface area, pore volume and average pore size of EMR and EMR-supported catalysts, as listed in Table 1. The BET surface area, pore volume and average pore size of EMR were determined to be 34 m^2 g^{-1}, 0.089 cm^3 g^{-1} and 10.6 nm, respectively. After loading metal oxides, sharp declines in the pore volume and the BET surface area were observed, which was ascribed to the penetration of the metal oxide particles into the pores of EMR. Moreover, the increase of average pore size after supporting metal oxides could be explained by the blocking of small pores by metal oxides and the collapse of the part of the small pores during calcination.

The surface characteristics of EMR and Co/EMR catalysts were studied using FTIR spectroscopy. As seen from Fig. 2, the stretching vibration of water O–H was indicated by the peak at 3432 cm^{-1}.[29] The strong peaks at 1642 cm^{-1} and 1450 cm^{-1} were attributed to M–O (M = Fe and Mn) vibration and Ca–O vibration, respectively.[30] The antisymmetric adsorption of Si–O and Si–O–Si was indicated by the peaks at 1121 cm^{-1}, 1030 cm^{-1}, 826 cm^{-1} and 673 cm^{-1}.[31] Furthermore, the peak located at 478 cm^{-1} was related to the external ring structure vibrations. The bridging of SiO_4 tetrahedra by oxygen atoms caused the formation of these ring structures.[32] Unfortunately, Co–O stretching signals were unobserved in the FTIR spectrum of Co/EMR.

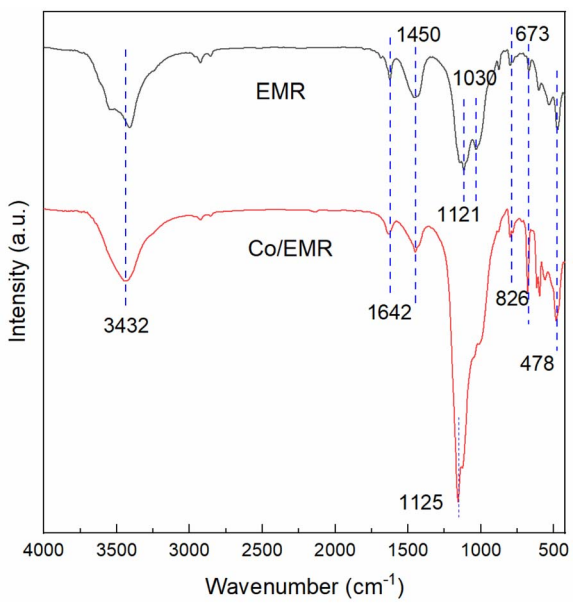

Fig. 2 FTIR spectra of EMR and Co/EMR.

The morphologies and microstructure of EMR and Co/EMR were displayed in SEM and TEM images. From the SEM image in Fig. 3a, EMR had a fairly smooth surface with a flat block morphology. After loading Co-oxides, many tiny particles were observed on the EMR surface in Fig. 3b. Moreover, the SEM images of other supported catalysts (Mn/EMR, Fe/EMR, Ce/EMR and Zn/EMR) are presented in Fig. S1 in the ESI.† No obvious changes were observed in the morphology after loading of metal oxides onto EMR. As seen from Fig. 3c, the TEM image which was in accordance with the SEM image also indicated that Co/EMR exhibited a block structure. The HRTEM image of Co/EMR in Fig. 3d showed a clear lattice fringe spacing of 0.255 nm, 0.152 nm and 0.466 nm, corresponding to the (110) plane of α-Fe_2O_3, (215) plane of Mn_3O_4, and (111) plane of Co_3O_4 respectively. Mn, Fe, O, Si, Mg, S, Al and Co elements were detected in the EDS spectrum of Co/EMR (Fig. 3e), suggesting that Co-oxides were successfully supported onto the EMR surface.

3.2. Removal of acetaminophen

3.2.1 Effect of active components supported on EMR. To evaluate the impact of active components supported on EMR, the adsorption and heterogeneous Fenton degradation of acetaminophen by EMR, Mn/EMR, Fe/EMR, Ce/EMR, Zn/EMR and Co/EMR were conducted. As shown in Fig. 4a, the adsorption had low removal ability for acetaminophen. For example, the pristine EMR presented the highest adsorption performance, just allowing an acetaminophen removal of 3.7% after 180 min of adsorption. Moreover, as seen from Fig. 4b, the degradation of acetaminophen by H_2O_2 alone was only 12.2%, implying that the removal of acetaminophen mainly depended on the heterogeneous Fenton oxidation. Among these EMR-supported catalysts, the worst catalytic activity (25.9% acetaminophen removal rate) was observed in Zn/EM, while Co/EMR exhibited the highest catalytic activity with a degradation rate of 63.8% for acetaminophen. Mn/EMR and Fe/EMR exhibited similar catalytic activity, and the activity of Ce/EMR was second only to that of Co/EMR.

The mineralization of acetaminophen was assessed by TOC analysis, as displayed in Fig. 4c. The TOC removal efficiency was less than the degradation rate of acetaminophen in all different systems, indicating refractory intermediate product formation during the degradation process. Only 6.1% of acetaminophen was mineralized by the oxidation of single H_2O_2. However, approximately 35.7% of acetaminophen molecules were decayed to H_2O and CO_2 after 480 min of reaction in the presence of Co/EMR. As discussed above, Co/EMR had the best catalytic effect in heterogeneous Fenton degradation of acetaminophen, so Co/EMR was used in the subsequent experiments of this study.

3.2.2 Effect of Co loading content. The loading content is one of the crucial factors for the catalytic performance of the supported catalyst. Therefore, the Co/EMR with different Co

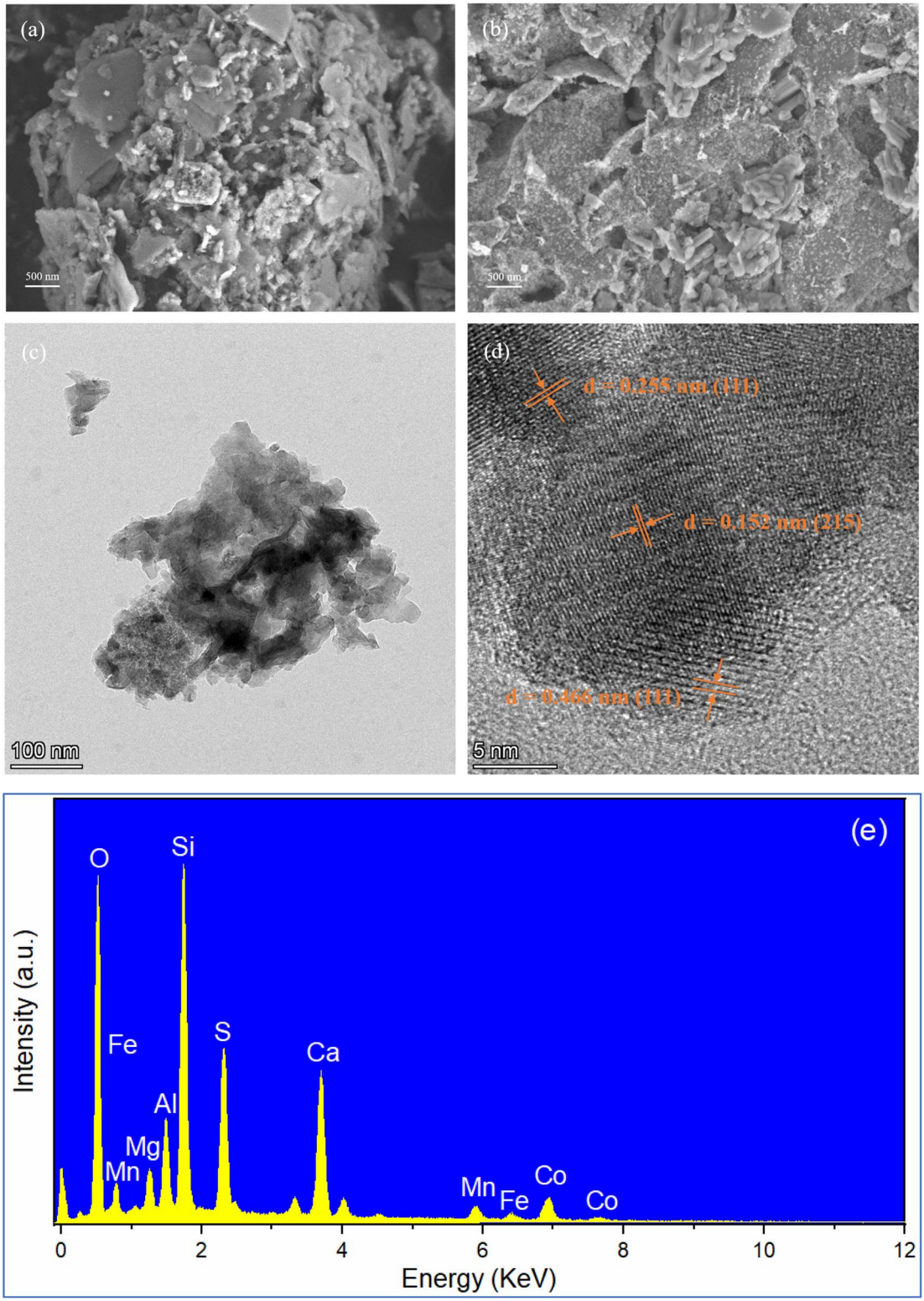

Fig. 3 SEM micrographs of EMR (a) and Co/EMR (b). TEM image (c), HRTEM image (d) and EDS spectrum (e) of Co/EMR.

loading contents were evaluated in the degradation of acetaminophen, and the results are depicted in Fig. 5. As the Co loading content increased from 1% to 5%, the acetaminophen degradation efficiency increased significantly, which indicated that Co oxides played an important part in heterogeneous Fenton degradation of acetaminophen. However, when the loading content was further raised from 5% to 9%, the acetaminophen degradation rate decreased from 63.8% to 39.1%.

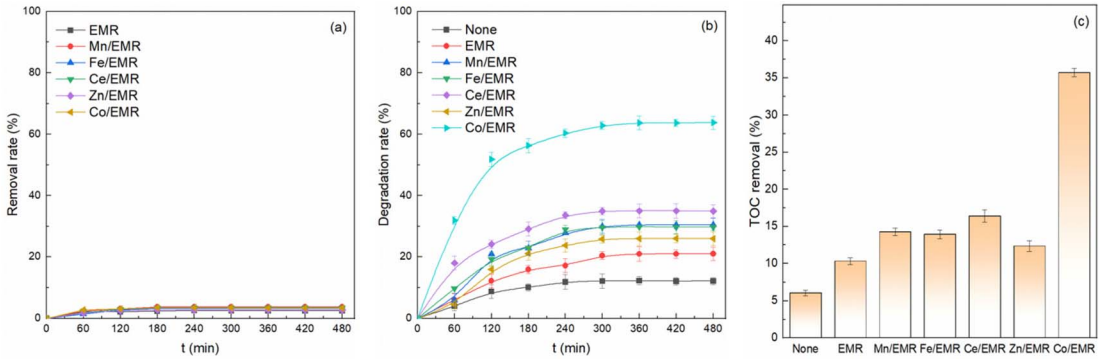

Fig. 4 (a) Adsorption of acetaminophen by EMR and EMR-supported catalysts, (b) acetaminophen degradation and (c) TOC removal in a heterogeneous Fenton process by EMR and EMR-supported catalysts. Reaction conditions: $[\text{acetaminophen}]_0$ = 10 mg L^{-1}, $[H_2O_2]_0$ = 307.9 mM, $[\text{catalyst}]_0$ = 1.0 g L^{-1}, initial pH = 6.98 (unadjusted), and T = 25 °C.

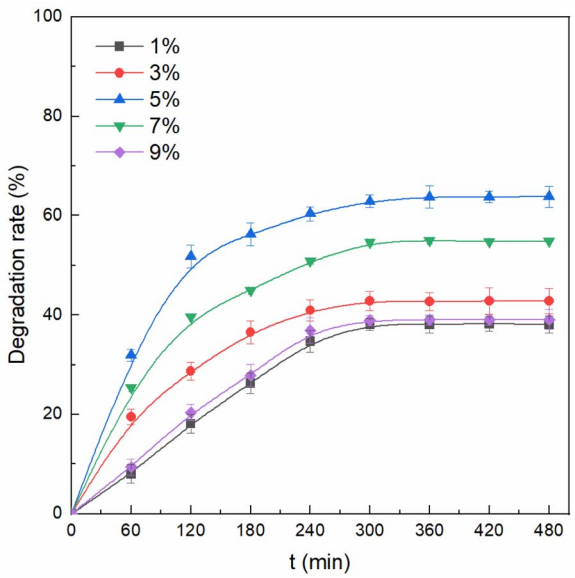

Fig. 5 Effect of Co loading content on the degradation of acetaminophen. Reaction conditions: $[\text{acetaminophen}]_0$ = 10 mg L^{-1}, $[H_2O_2]_0$ = 307.9 mM, $[\text{Co/EMR}]_0$ = 1.0 g L^{-1}, initial pH = 6.98 (unadjusted), and T = 25 °C.

Although the increase of Co loading content could provide more active sites for heterogeneous Fenton reaction, higher Co content might negatively affect the pore volume and surface area of the Co/EMR catalyst (Table 1) and the accumulation of active sites results in the inaccessibility of reactants. The above results showed that the optimal Co coating amount for heterogeneous Fenton degradation of acetaminophen was 5%.

3.2.3 Effect of reaction parameters. As shown in Fig. 6, the influence of diverse reaction parameters including catalyst dosage, H_2O_2 dosage and initial solution pH on the degradation of acetaminophen using Co/EMR as a heterogeneous Fenton catalyst was further investigated. As seen from Fig. 6a, by increasing the Co/EMR dosage from 0.5 to 1.0 g L^{-1}, the acetaminophen degradation rate after 480 min was improved from 21.5% to 63.8%. And only 39.2% of acetaminophen was decayed when using 2.0 g L^{-1} Co/EMR catalyst. It is well known that larger dosages of the catalyst could provide more active sites and thus generate more ROS, resulting in a higher degradation rate.[33] However, excessive catalyst existing in the reaction system would decrease the adsorption of H_2O_2 at the unit surface and reduce the utilization of H_2O_2.[34] And the produced ROS might also be scavenged by excessive metal species.[35] Therefore, the optimal dosage of the Co/EMR catalyst was 1.0 g L^{-1} in heterogeneous Fenton degradation of acetaminophen.

The influence of H_2O_2 dosage on acetaminophen degradation by Co/EMR was evaluated, and the results are depicted in Fig. 6b. When the H_2O_2 concentration was increased from 132.0 to 307.9 mM, the acetaminophen removal was increased accordingly from 9.5% to 63.5%. H_2O_2 was the source for the production of ROS, and more ROS would be generated by increasing the H_2O_2 concentration.[36]

The solution pH could influence the activity of the oxidant and substrate and the surface charge of the solid catalyst. Hence, the initial solution pH values of 3.34, 5.74, 6.98 (unadjusted), 9.99 and 11.13 were employed to study acetaminophen degradation. As presented in Fig. 6c, extremely alkaline or acidic solutions negatively affected acetaminophen degradation, while the acetaminophen removal was the highest under neutral conditions. The same results were also found in TOC removal (Fig. 6d). Excess acid could hinder the reaction of ROS, and thus affect the performance of the heterogeneous Fenton oxidation,[37] and H_2O_2 would rapidly decompose into O_2 and H_2O at extremely alkaline pH.[33] Fig. 6d also shows the final solution pH after the reaction was performed for 480 min. Initial pH values of 3.34, 5.74 and 6.98 resulted in a higher final pH, while initial pH values of 9.99 and 11.13 resulted in a lower final pH. This change in the solution pH might be mainly ascribed to the generation of intermediate products by the decay of acetaminophen during the reaction process.

3.3. Mechanism of reaction

3.3.1 Identifying ROS in the heterogeneous Fenton process. As illustrated in Fig. 7a, the ROS generated in the heterogeneous Fenton process and their roles in acetaminophen degradation were investigated by radical trapping

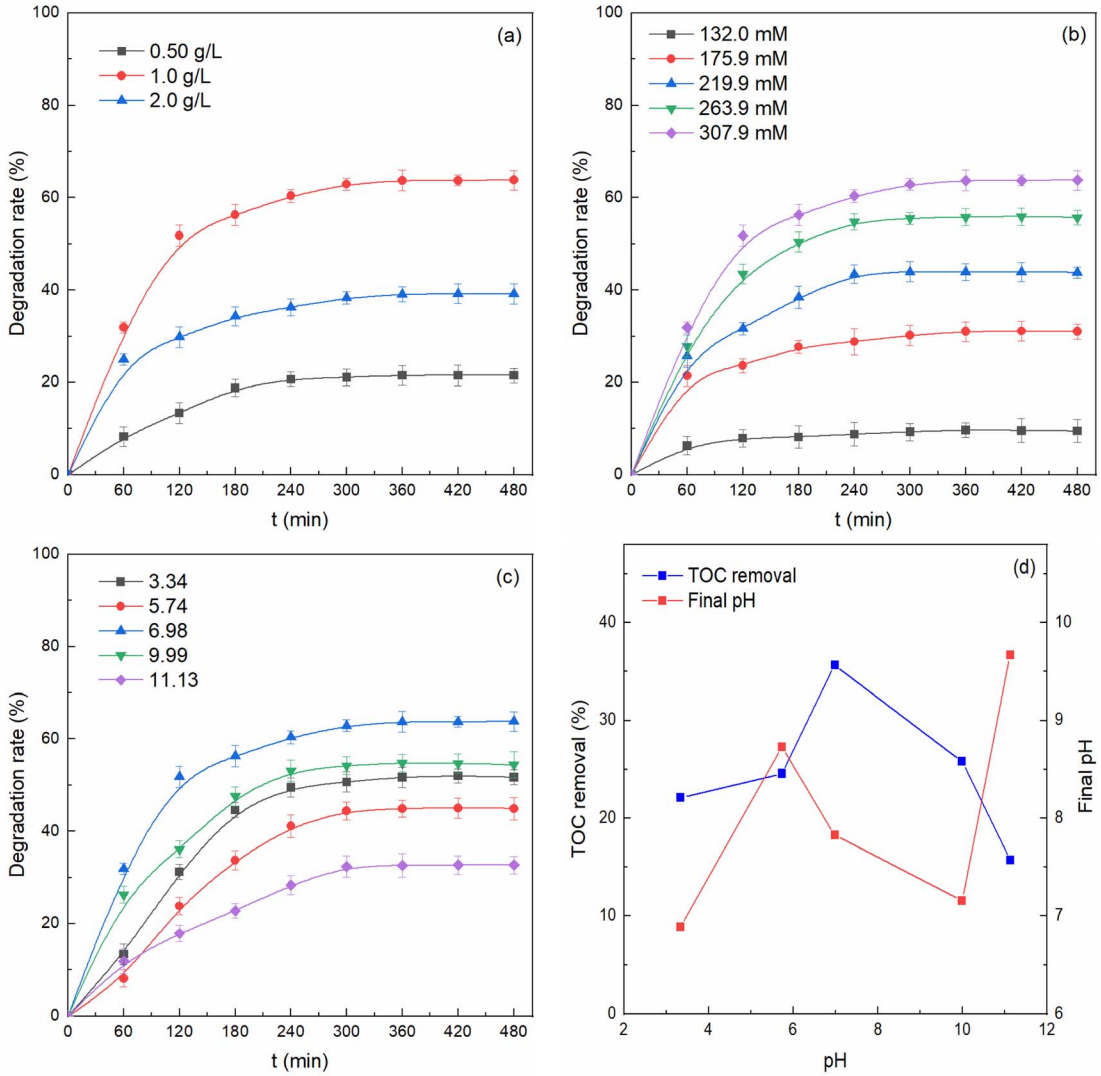

Fig. 6 Effect of reaction conditions on acetaminophen degradation through the heterogeneous Fenton reaction with Co/EMR: (a) catalyst dosage, (b) H_2O_2 dosage and (c) initial solution pH; (d) TOC removal and the final pH after the reaction. With the exception of the evaluated parameter, the reaction conditions were as follows: $[acetaminophen]_0 = 10$ mg L^{-1}, $[H_2O_2]_0 = 307.9$ mM, $[Co/EMR]_0 = 1.0$ g L^{-1}, initial pH = 6.98 (unadjusted), and $T = 25$ °C.

experiments.[38] In this study, *tert*-butanol (TBA) was used to capture $^{\bullet}OH$ and benzoquinone (BQ) was used to capture $O_2^{\bullet-}$. The degradation of acetaminophen was apparently inhibited when either TBA or BQ was introduced. In the presence of 10 mM TBA, the acetaminophen degradation efficiency declined from 63.8% to 39.5%, and 50 mM TBA led to a further decline to 19.9%. And the acetaminophen removal rate was decreased to 27.2% and 15.8% when using 10 mM and 50 mM BQ, respectively. Therefore, both $^{\bullet}OH$ and $O_2^{\bullet-}$ were generated in heterogeneous Fenton degradation of acetaminophen. It was noted that when the concentration of capture agents was raised from 10 to 50 mM, the acetaminophen degradation efficiency decreased by 19.6% for TBA and 11.4% for BQ. These findings suggested that $^{\bullet}OH$ contributed more than $O_2^{\bullet-}$ for the decay of acetaminophen.

EPR spectroscopy with DMPO was further conducted to confirm the presence of $^{\bullet}OH$ and $O_2^{\bullet-}$. As presented in Fig. 7b, DMPO-$^{\bullet}OH$ and DMPO-$O_2^{\bullet-}$ adduct signal peaks were observed, which verified the trapping experiment results that both $^{\bullet}OH$ and $O_2^{\bullet-}$ were the ROS for the heterogeneous Fenton degradation of acetaminophen. Besides, this signal intensity of both $^{\bullet}OH$ and $O_2^{\bullet-}$ increased as the reaction progressed, suggesting that these ROS continued to produce during the heterogeneous Fenton reaction.

3.3.2 Proposed degradation mechanisms. To unravel the degradation mechanism of acetaminophen, XPS analysis of Co/EMR before and after reaction was conducted. As shown in Fig. 8a, the Fe $2p_{3/2}$ orbital was deconvoluted into two peaks at 710.4 eV (ascribed to Fe^{II}) and 713.8 eV (ascribed to Fe^{III}).[39] The relative intensity of the Fe species changed after reaction, in which Fe^{II} declined from 64.4% to 40.1%, but Fe^{III} raised from 35.6% to 59.9%. For Mn 2p in Fig. 8b, the fresh Co/EMR in the Mn $2p_{3/2}$ orbital was fitted into two peaks at 641.3 eV and 643.3 eV, which could be related to Mn^{II} and Mn^{III},

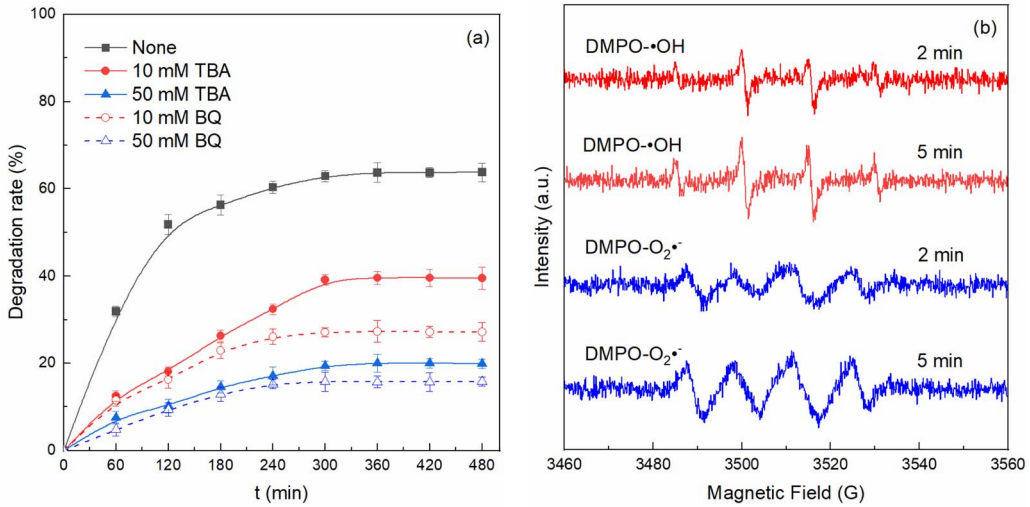

Fig. 7 (a) Impact of radical capture agents on the heterogeneous degradation of acetaminophen with Co/EMR; (b) EPR spectra of $^{\bullet}OH$ and $O_2^{\bullet-}$ at 2 min and 5 min. Reaction conditions: $[acetaminophen]_0$ = 10 mg L^{-1}, $[H_2O_2]_0$ = 307.9 mM, $[Co/EMR]_0$ = 1.0 g L^{-1}, initial pH = 6.98 (unadjusted), and T = 25 °C.

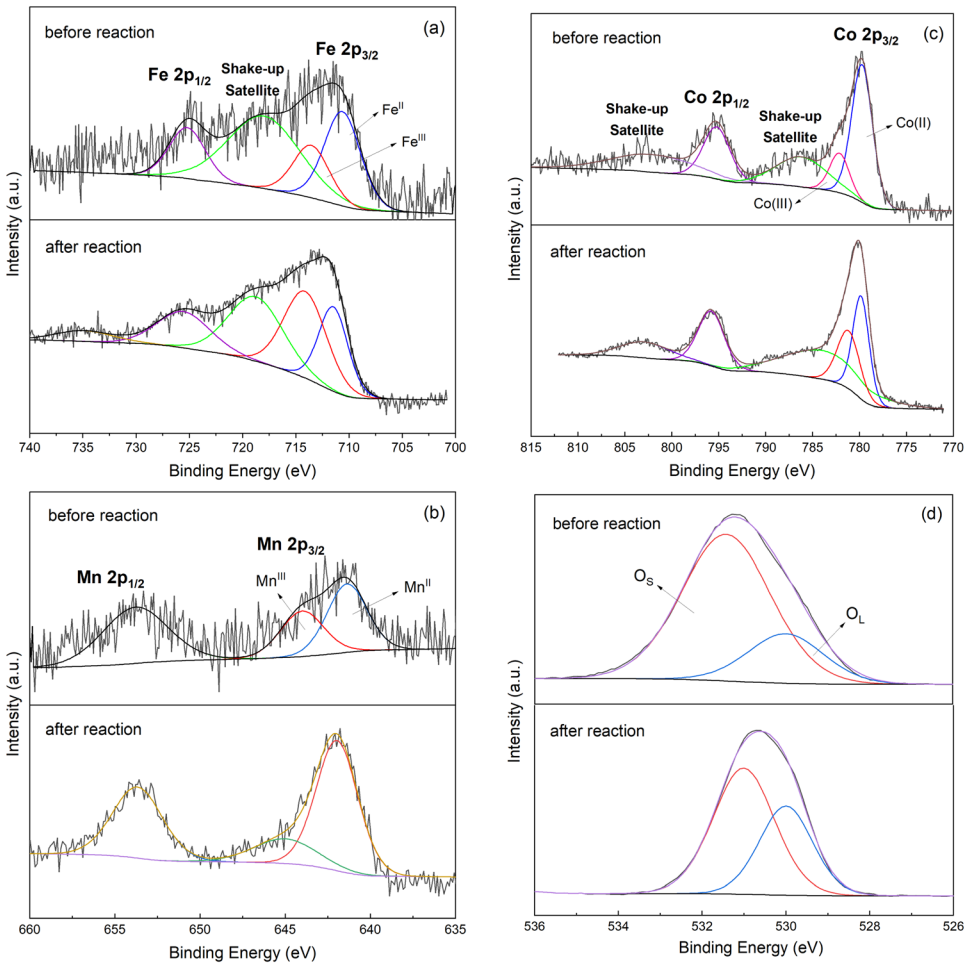

Fig. 8 XPS spectra of (a) Fe 2p, (b) Mn 2p, (c) Co 3d and (d) O 1s of the Co/EMR catalyst before and after the reaction.

respectively.[40] After oxidation, Mn^{II} content increased from 58.2% to 69.6%. As can be seen from the Co 2p XPS spectra in Fig. 8c, two peaks with the binding energies at 779.5 eV and 782.1 eV in the Co $2p_{3/2}$ orbital were ascribed to Co^{II} and Co^{III}, respectively.[41] After the heterogeneous Fenton reaction, the ratio of Co^{II}/Co^{III} changed from 3.73 to 1.29. The above results showed that Fe, Mn and Co were the active sites on the Co/EMR catalyst for acetaminophen degradation.

The O 1s spectra (Fig. 8d) showed peaks at 529.9 eV (assigned to lattice oxygen, O_L) and 531.4 eV (assigned to adsorbed oxygen or surface oxygen, O_S).[39] The O_S peak is also related to oxygen vacancies (O_v) because molecular oxygen was adsorbed on the surficial O_v.[42] The relative content of O_S slightly decreased from 77.6% to 62.1% after the catalytic reaction, signifying that the O_v on the surface of Co/EMR was also involved in the catalytic process. As illustrated in Fig. S2,† the EPR signal intensity of the O_v decreased after reaction, which further confirmed the important role of O_v in the catalytic process. The previous studies have proved that O_v on the catalyst surface could enhance the utilization rate of H_2O_2, increase electron transfer, and thus promote the formation of $^{\cdot}OH$.[38,43]

From the above analysis, the proposed mechanism for the degradation of acetaminophen is illustrated in Scheme 1. Firstly, H_2O_2 could be activated by the low valent Fe^{II}, Mn^{II} and Co^{II} ions on the Co/EMR surface to produce $^{\cdot}OH$ (eqn (1)–(3)). Then the high valent Fe^{III}, Mn^{III}, and Co^{III} ions could react with H_2O_2 to generate a large number of $^{\cdot}OOH$, as shown in eqn (4)–(6). The newly produced $^{\cdot}OOH$ could be transformed into $O_2^{\cdot-}$ according to the reactions in eqn (7) and (8) under different solution pH. Moreover, Fe^{II} could reduce Mn^{III} and Co^{III} due to the lowest standard reduction potential of Fe^{III}/Fe^{II} with 0.77 V (eqn (9) and (10)). And Co^{III} could also be reduced by Mn^{II} (eqn (11)), since the standard reduction potential of Co^{III}/Co^{II} is 1.92 V and that of Mn^{III}/Mn^{II} is 1.54 V. Besides, according to previous reports,[44,45] O_v could lead to the accelerated reduction of Fe^{III} to Fe^{II} (eqn (12)). The reactions between the redox pairs of Fe^{III}/Fe^{II}, Mn^{III}/Mn^{II} and Co^{III}/Co^{II} and the existence of O_v on the Co/EMR surface improved the efficiency of electron transfer, thus promoting the formation of ROS. After the reaction described above, acetaminophen was degraded to small molecule compounds or thoroughly mineralized into CO_2 and H_2O by these produced ROS (eqn (13)).

$$Fe^{II} + H_2O_2 \rightarrow Fe^{III} + {}^{\cdot}OH + OH^- \quad (1)$$

$$Mn^{II} + H_2O_2 \rightarrow Mn^{III} + {}^{\cdot}OH + OH^- \quad (2)$$

$$Co^{II} + H_2O_2 \rightarrow Co^{III} + {}^{\cdot}OH + OH^- \quad (3)$$

$$Fe^{III} + H_2O_2 \rightarrow Fe^{II} + {}^{\cdot}OOH + H^+ \quad (4)$$

$$Mn^{III} + H_2O_2 \rightarrow Mn^{II} + {}^{\cdot}OOH + H^+ \quad (5)$$

$$Co^{III} + H_2O_2 \rightarrow Co^{II} + {}^{\cdot}OOH + H^+ \quad (6)$$

$$^{\cdot}OOH + OH^- \rightarrow O_2^{\cdot-} + H_2O \quad (7)$$

$$^{\cdot}OOH \rightarrow O_2^{\cdot-} + H^+ \quad (8)$$

$$Fe^{II} + Mn^{III} \rightarrow Fe^{III} + Mn^{II} \quad (9)$$

$$Fe^{II} + Co^{III} \rightarrow Fe^{III} + Co^{II} \quad (10)$$

$$Mn^{II} + Co^{III} \rightarrow Mn^{III} + Co^{II} \quad (11)$$

$$Fe^{III} + O_v \rightarrow Fe^{II} + O_2 + OH^- \quad (12)$$

$$^{\cdot}OH/O_2^{\cdot-} + \text{acetaminophen} \rightarrow \text{degradation products} \quad (13)$$

3.4. Practical application prospect of the Co/EMR catalyst

Three consecutive cycle experiments were conducted to investigate the recyclability and stability of the Co/EMR catalyst for the degradation of acetaminophen. As displayed in Fig. 9a, acetaminophen degradation efficiency dramatically declined from 63.8% to 43.2% in the second cycle, and only 37.3% of acetaminophen was decayed in the third cycle. The decrease of catalytic activity could be explained by the masking of catalytic

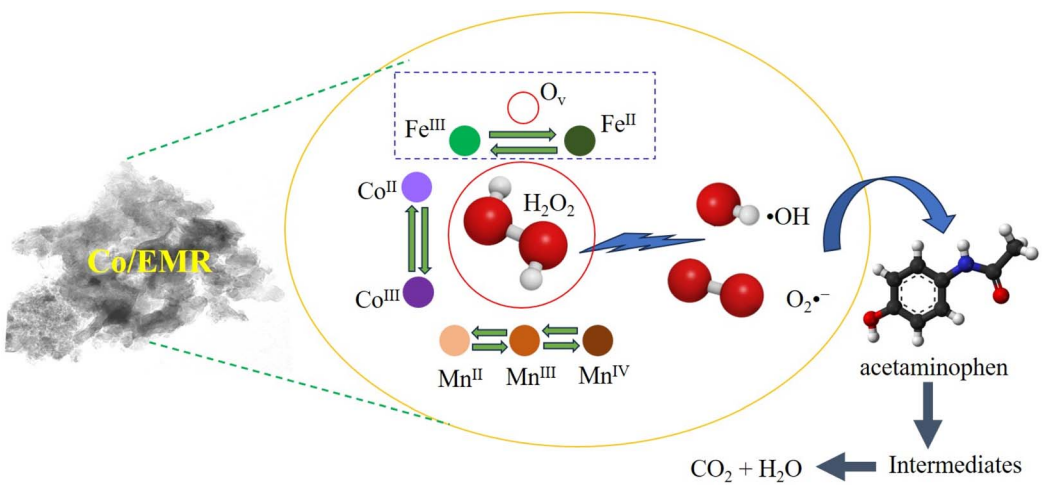

Scheme 1 Possible mechanisms of Co/EMR in the heterogeneous Fenton degradation of acetaminophen.

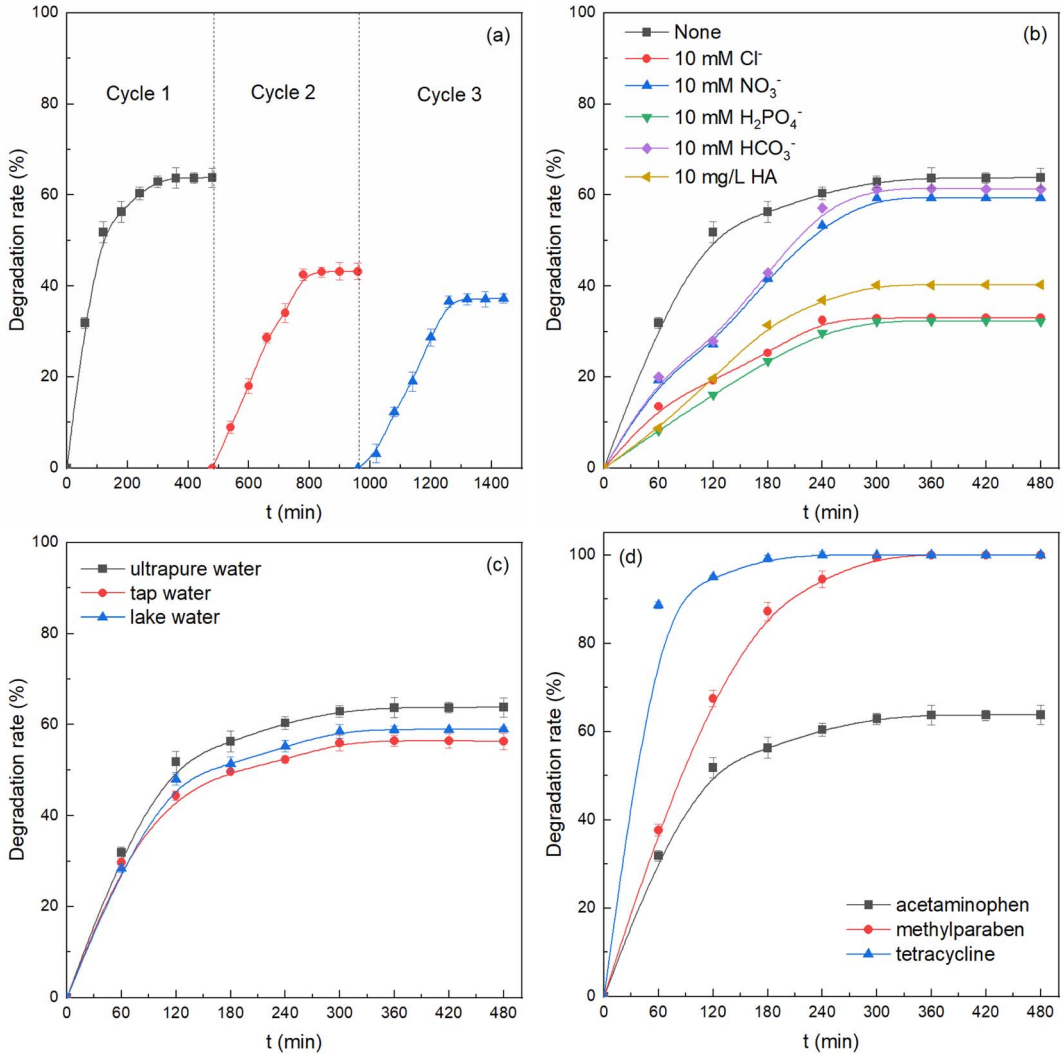

Fig. 9 (a) Reusability of the Co/EMR catalyst, (b) impact of coexisting species, (c) acetaminophen degradation in various water environments and (d) removal of various PPCPs. Reaction conditions: $[\text{pollutant}]_0 = 10$ mg L^{-1}, $[H_2O_2]_0 = 307.9$ mM, $[\text{Co/EMR}]_0 = 1.0$ g L^{-1}, unadjusted pH, and $T = 25$ °C.

reactive sites by the absorbed intermediate and the unavoidable loss of Co/EMR in the process of re-collecting the catalyst.[39] The concentration of the leached Co ions was 0.15 mg L^{-1} after three cycles, which was much lower compared to the emission standard of pollutants for copper, nickel, cobalt industry (1.0 mg L^{-1}) of China (GB 25467-2010).

Real wastewater contains various interference ions and dissolved organic matter (NOM), and the actual degradation performance of the heterogeneous Fenton process may be negatively affected by these interfering species. Herein, acetaminophen degradation was studied in the presence of several coexisting substances including Cl^-, NO_3^-, $H_2PO_4^-$, HCO_3^- and humic acid (HA). As presented in Fig. 9b, it was found that acetaminophen removal was seriously hampered by Cl^-, $H_2PO_4^-$ and HA, while NO_3^- and HCO_3^- showed slight influence on acetaminophen degradation. An acetaminophen degradation efficiency decline of 63.8% to 33.0% was observed in the presence of Cl^-, and a decline to 32.2% was observed with $H_2PO_4^-$. This could be attributed to the fact that $Cl^-/H_2PO_4^-$ ions could react with $^{\bullet}OH$ to form lower oxidative radicals such as $Cl_2^{\bullet-}/H_2PO_4^{\bullet-}$.[46] In addition, when HA was introduced into the system, the degradation rate of acetaminophen decreased to 40.3%, which might be due to the competition between acetaminophen and HA for the produced ROS.[46]

Besides, the degradation of acetaminophen in lake water (collected from the Mingde Lake in Tongren University, Tongren, China) and tap water was investigated to examine the adaptability of the Co/EMR catalyst to actual water environments. It could be seen from Fig. 9c that the acetaminophen degradation efficiency slightly decreased in both tap water and lake water. These results could be ascribed to the existence of organic matters in lake water and Cl^- ions in tap water. The Cl^- ions and organics would consume a part of ROS produced in the heterogeneous Fenton process.

In addition, to assess the general applicability of the Co/EMR catalyst in the heterogeneous Fenton process, methylparaben

and tetracycline were degraded under the same conditions. The methylparaben removal efficiency reached up to 99.4% within 300 min, while the degradation efficiency of tetracycline was almost 100% within 240 min (Fig. 9d). The results suggested that Co/EMR could be used as an effective heterogeneous Fenton catalyst for the treatment of other types of PPCPs. Moreover, the reaction conditions were not the optimal conditions for these pollutants, and the removal efficiency could further improve under optimal conditions in practical applications.

4. Conclusion

A series of supported catalysts were successfully synthesized in this work by using EMR as the support. The as-prepared catalysts were used in heterogeneous Fenton degradation of acetaminophen, and the results indicated that Co/EMR was the most effective for acetaminophen degradation, with a 63.8% degradation efficiency achieved within 480 min. Radical quenching experiments and EPR analysis confirmed that $^{\cdot}OH$ and $O_2^{\cdot-}$ were the dominant ROS during acetaminophen degradation. Reactions between the redox pairs of Fe^{III}/Fe^{II}, Mn^{III}/Mn^{II} and Co^{III}/Co^{II} and the existence of O_v on the Co/EMR surface improved the efficiency of electron transfer, and thus promoted the production of ROS in the heterogeneous Fenton process. Moreover, the Co/EMR catalyst showed a good adaptability to the actual water environment and a broad application to the removal of other pollutants. This heterogeneous Fenton system expands the horizon for the high-value utilization of EMR and shows potential for treating PPCPs in wastewater.

However, there are still some issues that should be solved in the future work. First of all, Co/EMR with the highest catalytic activity was used a heterogeneous Fenton catalyst, just showing a degradation rate of 63.8% for acetaminophen under the optimal experimental conditions. There is still room for improvement, and some techniques should be used to improve the catalytic performance of Co/EMR. Secondly, the reusability of Co/EMR is not so good, and it is imperative to find ways to partially restore the catalytic performance of Co/EMR.

Data availability

The corresponding author will provide access to all the data used to support this research upon receiving an adequate request.

Conflicts of interest

The authors declare that they have no conflicts of interest.

Acknowledgements

This work was financially supported by the National Natural Science Foundation of China (22166031, 22266030), Department of Education of Guizhou Province (QJJ[2022]055, QJJ[2022]003, [2023]026 and QJJ[2022]092), Guizhou Provincial Science and Technology Projects (QKHCG[2023]ZD008 and QKHJC-ZK[2023]YB459) and Tongren city Science and Technology Projects (TSKY[2023]70).

References

1 M. Sun, W. Fang, Q. Liang, Y. Xing, L. Lin and H. Luo, *J. Environ. Chem. Eng.*, 2024, **12**, 112647.
2 N. O. Sanjeev and A. E. Valsan, *J. Environ. Chem. Eng.*, 2024, **12**, 112649.
3 C. Xiao, Y. Hu, Q. Li, J. Liu, X. Li, Y. Shi, Y. Chen and J. Cheng, *Sci. Total Environ.*, 2023, **858**, 159587.
4 F. S. Mustafa and K. H. Hama Aziz, *Process Saf. Environ. Prot.*, 2023, **13**, 115–128.
5 W. Li, Q. Zhu, X. Yin, Z. Gao, K. Wei, S. Liu, X. Zhang, H. Chen, Y. Zhang and W. Han, *Sep. Purif. Technol.*, 2024, **335**, 126150.
6 S. Zhao, H. Li, J. Zhou, T. Sumpradit, E. Salama, X. Li and J. Qu, *Chem. Eng. J.*, 2024, **482**, 148979.
7 Y. Liu, S. Huang, H. J. Sun, Y. Liu, L. Liang, Q. Nan, T. Wang, Z. Chen, J. Tang, C. Hu and J. R. Zhao, *J. Sci.:Adv. Mater. Devices*, 2023, **8**, 100603.
8 H. D. Qin, H. Cheng, H. Li and Y. Wang, *Chem. Eng. J.*, 2020, **396**, 125304.
9 H. D. Qin, Y. C. Yang, W. Shi and Y. B. She, *Environ. Sci. Pollut. Res.*, 2021, **28**, 26558–26570.
10 H. D. Qin, Y. C. Yang, W. Shi, Y. B. She and S. Z. Wu, *J. Environ. Chem. Eng.*, 2021, **9**, 106184.
11 S. Z. Wu, H. D. Qin, H. Cheng, W. Shi, J. Chen, J. M. Huang and H. Li, *Catal. Commun.*, 2022, **171**, 106522.
12 L. Pang, D. Wang, H. Wang, M. An and Q. Wang, *Constr. Build. Mater.*, 2022, **330**, 127268.
13 Y. Luo, X. Zhou, Z. Luo, H. Ma, Y. Wei and Q. Liu, *Cem. Concr. Compos.*, 2022, **133**, 104653.
14 X. Shen, F. Yan, Z. Zhang, C. Li, S. Zhao and Z. Zhang, *Waste Manage.*, 2021, **121**, 354–364.
15 H. Chen, Q. Long, Y. Zhang, S. Wang and F. Deng, *Ecotoxicol. Environ. Saf.*, 2020, **194**, 110384.
16 S. He, D. Jiang, M. Hong and Z. Liu, *J. Cleaner Prod.*, 2021, **306**, 127224.
17 J. Wang, *Multipurp. Util. Miner. Resour.*, 2018, **2**, 115–118.
18 N. Wang, Z. Fang, S. Peng, D. Cheng, B. Du and C. Zhou, *Hydrometallurgy*, 2016, **164**, 288–294.
19 S. He, B. P. Wilson, M. Lundstrom and Z. Liu, *J. Hazard. Mater.*, 2021, **402**, 123561.
20 L. Luo, L. Jiang and N. Duan, *Environ. Eng.*, 2017, **35**, 139–143.
21 J. Pan, N. Xie, X. Ming, Y. Wang and H. Su, *J. Guangxi Univ., Nat. Sci. Ed.*, 2015, **40**, 551–557.
22 R. Liu, H. Wang, Z. Liu and C. Tao, *J. Water Process Eng.*, 2020, **38**, 101655.
23 D. Wang, Q. Wang and J. Xue, *Resour., Conserv. Recycl.*, 2020, **154**, 104645.
24 M. Song, J. Zhang, H. Yang, P. Zhou and Q. Zhang, *New Building Materials*, 2019, **9**, 133–137.
25 H. Zhou, P. Chen, Y. Zhao, R. Liu and J. Wei, *Concrete*, 2019, **10**, 97–99.
26 X. Li, H. Liu, Y. Zhang, J. Mahlknecht and C. Wang, *J. Environ. Manage.*, 2024, **352**, 120051.

27 J. Lan, Y. Sun, P. Huang, Y. Du, W. Zhan, T. C. Zhang and D. Du, *Chemosphere*, 2020, **252**, 126487.
28 M. Li, F. Huang, L. Hu, W. Sun, E. Li, D. Xiong, H. Zhong and Z. He, *Chem. Eng. J.*, 2020, **401**, 126085.
29 A. Palomo, M. Criado and A. Ferna, *Microporous Mesoporous Mater.*, 2007, **106**, 180–191.
30 C. Li, H. Zhong, S. Wang, J. Xue and Z. Zhang, *Colloids Surf., A*, 2015, **470**, 258–267.
31 W. R. Taylor, *Earth Planet. Sci.*, 1990, **99**, 99–117.
32 J. M. Hunt, M. P. Wisherd and L. C. Bonham, *Anal. Chem.*, 1949, **22**, 1478–1497.
33 J. Wang, C. Liu, J. Qi, J. Li, X. Sun, J. Shen, W. Han and L. Wang, *Environ. Pollut.*, 2018, **243**, 1068–1077.
34 R. X. Huang, Z. Q. Fang, X. M. Yan and W. Cheng, *Chem. Eng. J.*, 2012, **197**, 242–249.
35 X. Y. Zhang, Y. B. Ding, H. Q. Tang, X. Y. Han, L. H. Zhu and N. Wang, *Chem. Eng. J.*, 2014, **236**, 251–262.
36 M. Xia, M. C. Long, Y. D. Yang, C. Chen, W. M. Cai and B. X. Zhou, *Appl. Catal., B*, 2011, **110**, 118–125.
37 C. Zheng, C. Yang, X. Cheng, S. Xu, Z. Fan, G. Wang, S. Wang, X. Guan and X. Sun, *Sep. Purif. Technol.*, 2017, **89**, 357–365.
38 H. Jin, X. K. Tian, Y. L. Nie, Z. X. Zhou, C. Yang, Y. Li and L. Q. Lu, *Environ. Sci. Technol.*, 2017, **51**, 12699–12706.
39 M. Li, Z. He, H. Zhong, W. Sun, L. Hu and M. Luo, *Chem. Eng. J.*, 2022, **441**, 136024.
40 H. Shen, M. Luo, J. Wang, M. Li, Z. He, H. Zhong, W. Sun, M. Ye and Y. Tang, *Chem. Eng. J.*, 2023, **472**, 144915.
41 Y. Li, S. Ma, S. Xu, H. Fu, Z. Li, K. Li, K. Sheng, J. Du, X. Lu, X. Li and S. Liu, *Chem. Eng. J.*, 2020, **387**, 124094.
42 J. Lim, Y. Yang and M. R. Hoffmann, *Environ. Sci. Technol.*, 2019, **53**, 6972–6980.
43 P. Gao, X. Chen, M. Hao, F. Xiao and S. Yang, *Chemosphere*, 2019, **228**, 521–527.
44 S. Guo, H. Wang, W. Yang, H. Fida, L. You and K. Zhou, *Appl. Catal., B*, 2020, **262**, 118250.
45 S. Yang, Z. Huang, P. Wu, Y. Li, X. Dong, C. Li, N. Zhu, X. Duan and D. D. Dionysiou, *Appl. Catal., B*, 2020, **260**, 118129.
46 K. Wang, X. Lu, D. Wu and P. Xiao, *J. Environ. Chem. Eng.*, 2023, **11**, 111053.